

Advan. High Pressure Res. 3, 1-39
(1969)

| | |
|---|-----|
| x | |
| CHAPTER 4 | |
| Electrical Conductivity and Electronic Transitions at High Pressures | |
| N. H. MARCH | |
| I. Outline | 241 |
| II. Pressure Ionization and Electronic Transitions | 244 |
| III. Metallic Transitions at Lower Pressures | 254 |
| IV. Electrical Conductivity of Alkali Metals | 263 |
| V. Pressure-dependence of Band Structures of Simpler Metals | 267 |
| VI. Excitonic Phases: Transcending Band Theory | 280 |
| VII. Effect of Pressure on Transition Temperatures of Cooperative Phenomena | 290 |
| VIII. Alloy Systems | 298 |
| IX. Speculations on Crystal Structures in Extreme High Pressure Regime | 303 |
| X. Concluding Remarks | 304 |
| References | 305 |
| Appendix I. Velocity of Sound in Metals and Metallic Alloys | 308 |
| A. Non-linear plasma | 308 |
| B. Extension of Bohr-Staver formula for liquid metal alloys | 309 |
| Appendix II. Analogy between Excitonic Phase and Superconducting State | 311 |

| | |
|--|-----|
| CHAPTER 5 | |
| Adsorption of Gases at High Pressures | |
| P. G. MENON | |
| I. Introduction | 313 |
| II. Experimental Methods | 316 |
| III. Results | 335 |
| IV. Adsorption Equilibria in Multicomponent Gas Mixtures | 350 |
| V. Miscellaneous | 359 |
| References | 363 |
| AUTHOR INDEX | 367 |
| SUBJECT INDEX | 379 |

CHAPTER 1

High Pressure Mössbauer Studies†

H. G. DRICKAMER, S. C. FUNG and G. K. LEWIS, JR.‡

Department of Chemistry and Chemical Engineering, and Materials Research Laboratory, University of Illinois, Urbana, Illinois, U.S.A.

| | |
|--|----|
| I. Introduction | 1 |
| II. Pressure Effects | 11 |
| A. Isomer shift | 11 |
| B. Quadrupole splitting | 19 |
| C. Magnetism | 23 |
| D. The measurement of f number | 26 |
| E. Conversion of Fe^{III} to Fe^{II} | 29 |
| F. High pressure Mössbauer studies on glass | 34 |
| References | 38 |

I. INTRODUCTION

The existence of the Mössbauer Effect (that is recoilless resonant radiation) was first discovered in 1958 (Mössbauer, 1958a, b). The principles involved have been reviewed in detail in the literature (Frauenfelder, 1963; Wertheim, 1964), so they will only be outlined here.

When a radioactive atom decays by gamma ray emission, the nucleus goes from an excited state to the ground state, and the energy of the gamma ray is a measure of the energy difference between these states. Consider first the case of a free atom. The emitted gamma ray will have associated with it a certain momentum, and in order to conserve momentum the atom must recoil. However, this recoil has associated with it kinetic energy which must reduce the energy of the gamma ray; the act of absorption of a gamma ray by a nucleus involves the inverse process. Thus the emission and absorption processes are not in resonance.

If, however, one fixes the atom in a crystal, the situation may be

† This work was supported in part by the United States Atomic Energy Commission under Contract AT(11-1)-1198. ‡ Present Address: Eastern Laboratories, E. I. duPont Company, Gibbstown, New Jersey, U.S.A.

altered. The energy and momentum can be considered as decoupled; the recoil momentum is transferred to the crystal as a whole and, if this is fixed in the laboratory, to the earth. The velocity of recoil, and hence the kinetic energy, is effectively zero. The vibrational energy of the lattice is quantized; if the lowest allowable quantum of vibrational energy (the lowest phonon energy) is large compared to the recoil energy, there will be a finite probability of recoilless decay. Since this energy peak is not Doppler broadened, it is nearly monochromatic, and the lower limit to the width is set by the lifetime of the excited state and the uncertainty principle. In actual cases there is usually additional broadening due to imperfect motion and other instrumental problems, relaxation phenomena, and other factors.

A wide variety of nuclei display Mössbauer resonance, but by far the most useful from the standpoint of the study of solids is ^{57}Fe . The process by which the 14.4 keV Mössbauer gamma ray is produced is outlined in Fig. 1(a), and in this paper we shall limit ourselves to studies involving this isotope.

The Mössbauer effect is capable of giving information concerning a

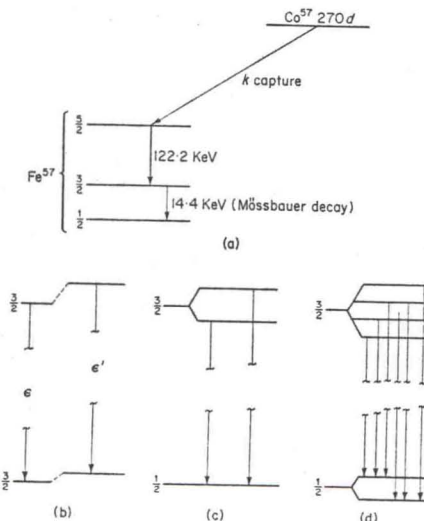


FIG. 1. Basic concepts for ^{57}Co - ^{57}Fe Mössbauer system. (a) ^{57}Co decay, (b) isomer shift, (c) electric field, (d) magnetic field.

number of different aspects of the nuclear environment. First and most basic is the isomer shift. The process of decay by gamma emission involves a transition of the nucleus from an excited state to its ground state. The difference in energy between these states is slightly but measurably perturbed by the electronic environment of the nucleus. Specifically, it is affected by those electronic wave functions having non-zero amplitude at the nucleus; and these must be states of zero angular momentum (*s* states). The electronic configuration of atomic iron is $1s^2 2s^2 2p^6 3s^2 3p^6 3d^6 4s^2$. The 1s and 2s wave functions surely have significant amplitude at the nucleus, but they are largely isolated from the surrounding atoms and can tell us little about changes in the environment. The 4s electrons interact strongly with the neighbouring atoms, and while they are largely shielded from the nucleus, they contribute significantly to studies of isomer shift changes, particularly in metals. In ionic states of iron the 4s levels are usually assumed to be sparsely occupied. The 3s electrons do not interact to any extent with the surrounding atoms or ions, although they have their radial maximum at very nearly the same point as the 3d electrons which do interact with the neighbouring atoms. Changes in the 3d states with changing environment will then affect the degree of shielding of the 3s electrons from the nucleus, which will be reflected in changes in the observed difference in nuclear energy levels, that is in the isomer shift (see Fig. 1(b)). Thus, a dilute solution of ^{57}Co (^{57}Fe) in copper will not be in resonance with ^{57}Fe dissolved in chromium, or with ^{57}Fe in FeCl_2 . If one now imparts a motion to the source with respect to the absorber, when the Doppler velocity just compensates for the difference in the isomer shifts of the two materials, resonance is obtained. A Mössbauer spectrometer is a device for measuring the velocities necessary to obtain resonance, and the differences in value of the isomer shift, $\Delta\epsilon$, in different environments is expressed in terms of the relative velocity necessary to obtain resonance. Spectrometers are widely described in the literature (Frauenfelder, 1963; Wertheim, 1964; also for high pressure, Pipkorn *et al.*, 1964; DeBrunner *et al.*, 1966), and will not be discussed here. For ^{57}Fe the energy differences (that is isomer shift differences) from material to material are of the order of a mm/sec or a fraction thereof. It is perfectly practical to measure differences smaller than 0.1 mm/sec, which corresponds to a thermal energy difference of 10^{-5}°C , or $\sim 10^{-5}$ calories ($\sim 10^{-9}$ eV) which illustrates the sensitivity of the technique.

The isomer shift is described by the equation:

$$\Delta\epsilon = \alpha[\psi_0^2(0) - \psi_A^2(0)] \quad (1)$$

where

$$\alpha = \frac{2}{3} \pi Z e^2 [R_E^2 - R_G^2] \approx \frac{2}{3} \pi Z e^2 [R \Delta R] \quad (2)$$

which for iron = $3.52 \times 10^{10} (R \Delta R)$.

Here the $\psi^2(0)$ are the amplitudes of the wave functions of the source and absorber at the nucleus, and R_G and R_E are the radii of the nucleus in the ground and excited state. From the standpoint of nuclear physics the value of ΔR is of considerable interest; from the viewpoint of solid state structure and electronic behaviour, the changes in $\psi_s^2(0) - \psi_s^2(0)$ with changing conditions are of paramount importance.

The nuclear energy levels can be perturbed by an electric field gradient at the nucleus. The ground state of spin one-half will remain unsplit, but the excited state of spin three-halves will split into two levels as indicated in Fig. 1(c). Under these conditions two transitions are possible, and one sees two peaks. The size of the splitting is then a measure of the electric field asymmetry seen by the nucleus. As will be discussed later, this effect gives important information concerning the local symmetry at the ^{57}Fe site, and the distribution and spin states of the electrons in the partially filled 3d shell.

A magnetic field at the iron nucleus also interacts with the nuclear levels of iron, splitting the excited level into four states and the ground level into two. When the selection rules ($\Delta m = 0, \pm 1$) are applied, one sees that a six line spectrum results as is shown in Fig. 1(d). The splittings between pairs of lines measures the magnetic field strength at the nucleus. It is thus possible to study changes in magnetic field with changing temperature, pressure, and chemical environment.

Finally, we have said that the phonon spectrum of the lattice determines the probability of recoilless decay, so that from the measured fraction of recoilless decays (proportional to the area under the Mössbauer peak) one can gain information about the lattice dynamics in the neighbourhood of the iron atom or ion. A number of rather sophisticated treatments have been given (Maradudin, 1966; Housley and Hess, 1966), but in this paper only the Debye approximation will be briefly considered where the recoilless fraction f is related to the characteristic temperature θ_D by:

$$f = \exp \left[-\frac{6E_r}{k\theta_D} \left(\frac{1}{4} + \left(\frac{T}{\theta_D} \right)^2 \int_0^{\theta_D/T} \frac{xdx}{e^x - 1} \right) \right] \quad (3)$$

where E_r is the recoil energy of the free nucleus due to decay.

Transition metal ions in crystals will be considered in this paper and it is therefore desirable to review qualitatively some of the features of

ligand field and molecular orbital theory. These theories are discussed in detail in various literature (Griffith, 1964; Orgel, 1960; Ballhausen, 1962; Ballhausen and Gray, 1965).

The five 3d energy levels on a free transition metal ion are all degenerate. A 3d electron on such an ion may be in its ground state or in an excited state. The energy difference between these states can be expressed in terms of the Condon-Shortley parameters or more conveniently in terms of the Racah parameters A, B, C (see Fig. 2). These parameters can be calculated in principle, but are usually evaluated from atomic spectra; they depend on the repulsion among the 3d electrons on the ion.

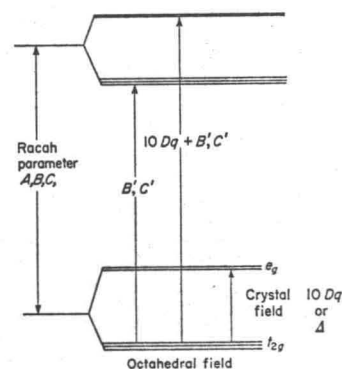


FIG. 2. Crystal field splittings and energies—octahedral symmetry.

If the ion is inserted into a crystal lattice, the surrounding ions provide a field of less than spherical symmetry. In this paper we shall discuss primarily octahedral symmetry wherein six ligands are arranged at the centres of the faces of a cube which has the iron at its centre, but we shall occasionally introduce the tetrahedral arrangement, where the ligands are at the corners of a regular tetrahedron surrounding the iron.

As seen in Fig. 2, these symmetries partially remove the degeneracy of the 3d levels. In octahedral symmetry the levels labelled t_{2g} (d_{xy}, d_{xz}, d_{yz}) lie below those labelled e_g ($d_{z^2}, d_{x^2-y^2}$); in tetrahedral symmetry this order is reversed.

The amount of splitting between these groups of levels depends on the intensity of the field supplied by the nearest neighbour ions (the

ligands) in the crystal. For historical reasons this energy difference is usually called $10 Dq$.

So far only arguments which depend on symmetry have been used. If one wishes to make even semiquantitative calculations, molecular orbitals combining realistic ligand and metal ion wave functions must be used to give orbitals which satisfy the symmetry requirements. Ballhausen and Gray have given a description of the process. A diagram such as Fig. 3 results, in which we see the combination of ligand

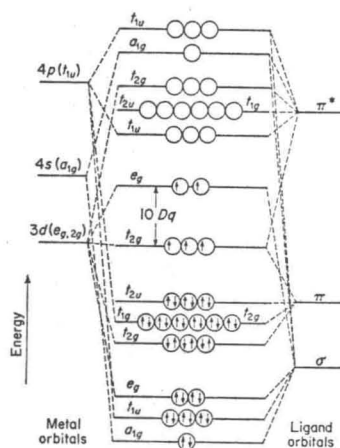


FIG. 3. Molecular orbital diagram—octahedral symmetry.

and metal ion wave functions to give bonding orbitals such as a_{1g} and t_{1u} , non-bonding orbitals such as t_{2u} , and anti-bonding orbitals such as t_{2g} and e_g . The separation between these last two is still a measure of the crystal field ($10 Dq$).

The $3d$ shell of iron is only partially filled. In the ideal case, the ferrous ion has six and the ferric ion five $3d$ electrons. There is more than one way to put the electrons in the levels; according to Hund's rule of atomic spectroscopy, the state of maximum spin should be lowest in energy. This case is illustrated in (a) and (b) of Fig. 4, and applies to most ionic materials. If the metal-ligand interaction is strong enough, energy may be saved by pairing spins as in (c) and (d). Potassium ferrocyanide and potassium ferricyanide are examples of this situation. For high spin ferric (a) and low spin ferrous (d) ions,

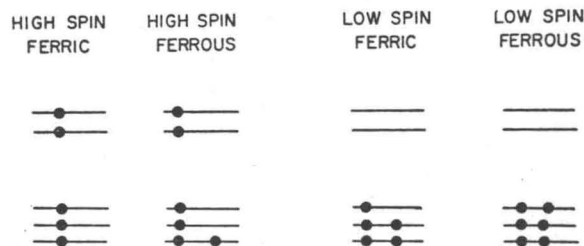


FIG. 4. Spin free and spin paired electron distributions for ferric and ferrous systems.

the $3d$ electrons present a field of spherical symmetry at the nucleus. For high spin ferrous and low spin ferric ions a strong probability of an asymmetric field exists. This is very important in understanding many aspects of quadrupole splitting.

A variety of different transitions are observed optically in crystals containing transition metal ions. There are $d-d$ transitions which measure $10 Dq$, or the Racah parameters B and C , or combinations of these two effects. These are of moderate intensity because they are allowed only due to vibrational interaction. Typically, $10 Dq$ is of the order of $5000-15,000 \text{ cm}^{-1}$ ($0.6-1.8 \text{ eV}$, $15-45 \text{ kcal}$) at one atmosphere. The combination peaks measuring both $10 Dq$ and B and C lie at somewhat higher energies, in the visible or near ultraviolet.

It is also possible to observe optical transitions which measure an electron transfer from a ligand level (t_{2u}) to a predominantly metal level (t_{2g}). This is an allowed transition and very intense, and the energy peak for such transitions typically lie at $25,000-40,000 \text{ cm}^{-1}$ ($3-5 \text{ eV}$), but they are broad, and the low energy tail sometimes extends through the visible and even into the infrared.

The effects of pressure on these transitions have been reviewed extensively elsewhere (Drickamer, 1963, 1965). In general, there is a marked increase in $10 Dq$ with pressure ($10-15\%$ in 100 kb). In the simplest order of theory, one would expect the crystal field to increase as R^{-5} , where R is the metal-ligand distance, and this is roughly what occurs. There is a measurable decrease in the Racah parameters with increasing pressure— $7-11\%$ in 100 kb . Apparently the $3d$ orbitals expand by interaction with the ligands, and this increases the average distance between electrons in the $3d$ shell, which reduces the repulsion between them.

The charge transfer peaks shift strongly to lower energy with increasing pressure, by as much as one half to 1 eV in 100 kb . This lowering

of the metal energy levels vis-à-vis the ligand is apparently due primarily to the spreading of the $3d$ orbitals mentioned above. It can be shown (Vaughan, 1968) that it is possible in principle to reduce this difference by several electron volts using this mechanism. A second factor which tends to stabilize the t_{2g} orbitals is an increase in π bonding of these orbitals with excited ligand orbitals. Since the π bonding is usually considerably smaller than the σ bonding at one atmosphere, it could be expected to increase relatively more. Lewis and Drickamer (1968a) have shown that this is probably a significant factor, but not the controlling one. All of these observations will be important in the interpretation of various aspects of high pressure Mössbauer spectra for iron in ionic and covalent compounds.

To understand the Mössbauer spectrum of iron metal and of iron as a dilute solute in transition metals, a knowledge of the band structure of these materials is important. A review of even simple band structure is beyond the scope of this article, and the transition metals are far from simple, as the relevant electrons are neither completely bound nor almost free. There is, however, evidence (Slater, 1965) that all of the b.c.c. transition metals have very similar band structure, while the close packed members of the series (especially the f.c.c. metals) are very much like each other, but significantly different from the b.c.c. metals. In both cases the conduction band has a mixture of $3d$ and $4s$ character, with different emphasis in different parts of reciprocal lattice space. The relative degree of s and d character may change with pressure. We shall here assume that Stern's (1955) calculations for iron are qualitatively correct.

In the study of magnetism in transition metals, the controversy as to whether the magnetic electrons are primarily tightly bound or itinerant is a long and complex one, with outstanding proponents on each side. High pressure Mössbauer studies have so far contributed in only a minor way to the solution of this problem.

Figure 5 shows the range of isomer shifts for ^{57}Fe in different environments, relative to metallic b.c.c. iron. According to the convention used, the larger the isomer shift, the lower the electron density at the nucleus. Several facts are immediately evident.

(1) Iron as a dilute solute in a series of transition metals shows a relatively narrow range of isomer shifts although the solvent atoms have from 1–9 d electrons in their outer d shell—this would indicate that $3d$ electrons of the iron are not completely integrated into the solvent d band, although, as shall be seen later, they are closely associated with it.

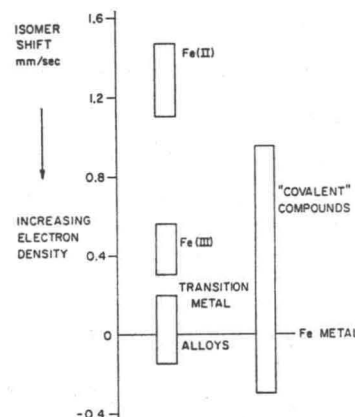


FIG. 5. Isomer shift ranges for iron and compounds.

(2) Ferrous ions typically exhibit a very low electron density. Since their outer configuration is nominally $3d^6 4s^0$, this can be attributed to the shielding of the $3s$ electrons by the $3d$.

(3) Ferric ions exhibit a significantly higher electron density than do ferrous ions. In both cases typical compounds fall in a range of electron densities, but the two ranges do not come close to overlapping. The ranges shown cover almost all the high spin compounds from the essentially completely ionic such as the fluorides to those with large covalent components such as the acetylacetonate, as long as they can be classified as ferrous or ferric. There is evidence that ferric compounds are generally more covalent than ferrous, and this would indicate some back donation from the ligands to the metal, so that the traditional $3d^5 4s^0$ ferric configuration is an oversimplification. In view of the narrow range of isomer shifts exhibited by the ferric compounds, however, the viewpoint taken here is that the major difference between the observed ferrous and ferric electron densities (~ 0.9 mm/sec) is due to the reduced shielding of the $3s$ electrons in the latter case.

(4) While the classification "covalent" is ambiguous in that all compounds exhibit some covalency, there are a number of compounds which involve a very high degree of electron sharing. Such compounds as ferrocene and potassium ferro- and ferricyanide fit this description. In addition there are compounds like FeSe_2 , FeTe_2 , FeP , FeP_2 , FeAs

and FeSb to which it is difficult to assign a definite valence. As one might expect, this rather amorphous group of compounds has a large range of isomer shifts.

Ingalls (1967) found a linear correlation between the maximum of the square of the radial portion of the $3d$ wave function and the $3s$ electron density at the nucleus using Hartree-Fock free ion wave functions. A variational calculation, the purpose of which was to establish the effect of change of the shape of the $3d$ orbitals in going from the free ion to the metal on the $3s$ density at the nucleus, indicates that the correlation is still good for the bond wave functions, even though some of these have large electron densities in the tail of the wave function.

Thus, in trying to interpret isomer shift data in terms of covalency, it is necessary to remember that the isomer shift may not be sensitive to electron density located between the metal ion and the ligand, which is a usual criterion for covalency, but primarily to the change of $3d$ density on the ion.

As was indicated earlier in the paper, the measured difference in isomer shift between source and absorber involves a constant α . There has been a considerable controversy about the value of α , and thus of $\Delta R/R$, although it is agreed that α is negative, that is that the radius of the nucleus in the excited state is less than that in the ground state. Walker *et al.* (1961) assigned the difference in isomer shift between ferrous and ferric ion entirely to the difference in shielding of the $3s$ electrons due to the presence of one more $3d$ electron (that is they assumed configurations $3d^6 4s^0$ and $3d^5 4s^0$). Using Watson's (1959) free ion wave functions they obtained the value

$$\alpha = -0.47 a_0^3 \text{ mm/sec} \quad (4)$$

where a_0 is the Bohr radius.

Simanek and Stroubec (1967) however assign the difference in isomer shift between ferrous and ferric ion entirely to a difference in occupation of the $4s$ level, that is they assume that the ferrous ion, at least in compounds like the fluoride, is completely ionic, while the ferric ion has the configuration $3d^5 4s^0$. They consider overlap distortion as the only significant factor in changing $\Delta\epsilon$ with pressure, and, using published data on the oxide and fluoride, obtain a considerably smaller value of about -0.12 for α .

Gol'danski (1963) and Danon (1966) also estimate a relatively small value for α . The value of α must be considered in discussing the effect of pressure on the isomer shift in metallic iron, and in iron as a dilute solute in transition metals.

II. PRESSURE EFFECTS

A. ISOMER SHIFT

The factors which affect the electron density at the nucleus as a function of pressure (interatomic distance) are of two types: (a) deformation of the wave functions, and (b) transfer of electrons between orbitals. This can take the form of transfer of electrons between, say, the $3d$ and $4s$ orbitals of an iron atom or ion, or transfer of electrons between the $3d$ and $4s$ parts of the conduction band of a metal, or of transfer of electrons between metal and ligand orbitals, either bonding or non-bonding. The process by which the electron density changes with interatomic distance is a complex one, so that any description given here is, at best, an approximation and must be regarded as tentative. We shall first discuss metals and alloys for which at least a reasonably quantitative theory has been developed, and then discuss the significant factors governing the behaviour of compounds.

1. Iron and Alloys

The isomer shift of ^{57}Fe in b.c.c. iron has been investigated by a number of people including Pound *et al.* (1961), Nicol and Jura (1963), Pipkorn *et al.* (1964), and Moyzis and Drickamer (1968a). Figure 6 is a composite of results, largely from the last two papers. The isomer shift decreases with increasing pressure, corresponding to an increase of

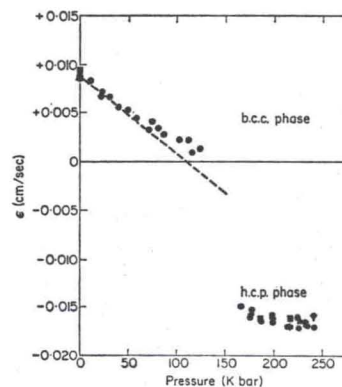


FIG. 6. Isomer shift of metallic iron versus pressure.

electron density at the nucleus, but the rate of increase decreases markedly at high pressure. As Moyzis has shown, $\Delta\epsilon$ is not linear in either pressure or volume. The experimental results can be expressed in the form:

$$\Delta\epsilon = -8.1 \times 10^{-4}P + 1.65 \times 10^{-6}P^2 \quad (5a)$$

$$= 1.38 \frac{\Delta V}{V} + 2.7 \left(\frac{\Delta V}{V} \right)^2 \text{ (mm/sec)} \quad (5b)$$

where P is in kb.

At about 130 kb there is a first-order phase transition in iron from the b.c.c. to the h.c.p. structure, with a large decrease in isomer shift of the order of -0.24 mm/sec. The isomer shift in the high pressure h.c.p. phase decreases relatively slowly with increasing pressure or density, which, as shall be seen, is characteristic of close-packed metals.

Figures 7-9 show the isomer shift for iron as a dilute solute in a series of transition metals, plotted versus $\Delta V/V$ for the host. The solid line

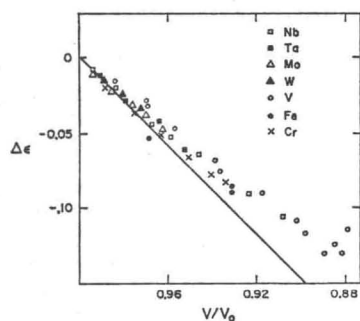


FIG. 7. Isomer shift versus $\Delta V/V$ —b.c.c. metals.

represents the low pressure slope for b.c.c. iron. In Fig. 7 are shown the b.c.c. metals and in Figs 8 and 9 close-packed systems. These results are from the work of Pipkorn *et al.* (1964), Edge *et al.* (1965), Drickamer *et al.* (1965), and Moyzis and Drickamer (1968b). The feature which is immediately apparent is that the change of isomer shift with compression is much greater in the former than in the latter.

Ingalls (1967) has presented an analysis of the isomer shift of iron which can also be applied qualitatively to the dilute alloys (Ingalls *et al.*, 1967; Moyzis and Drickamer, 1968a, 1968b).

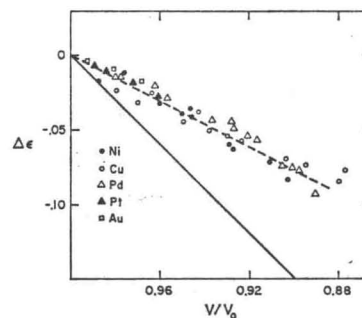


FIG. 8. Isomer shift versus $\Delta V/V$ —f.c.c. metals.

In iron the $4s$ electrons exist in a relatively broad band, such that they can be characterized as "nearly free". This overlaps the much narrower $3d$ band. The other transition metals have a qualitatively similar structure, but within each group, b.c.c., f.c.c. and h.c.p., the similarities are much stronger than they are between groups.

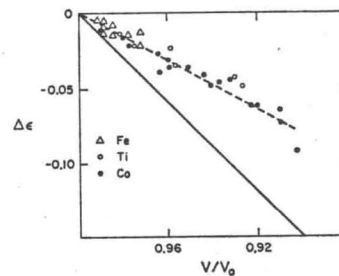


FIG. 9. Isomer shift versus $\Delta V/V$ —h.c.p. metals.

In the first order, one can divide the effects of changing pressure (or volume) into two parts: the effect of compression of the $4s$ band $d(\Delta\epsilon)_L$, and the effect of transfer of electrons into or out of s -like states in the s - d conduction band $d(\Delta\epsilon)_B$. From the calculations of Walker *et al.* (1961) one can estimate the first effect:

$$\frac{d(\Delta\epsilon)_L}{d \ln V} = 1.4 \text{ mm/sec.} \quad (6)$$

Since we are interested in the pressure dependence of $|\psi(0)|^2$, only the 4s and 3s electron contributions are considered. The 4s electrons are affected in a direct way since they are itinerant and thus can be expected to scale with volume. The 1s, 2s, and 3s electrons are not directly affected by small volume changes but the 3s electrons are indirectly affected by the changes in 3d electron wave functions.

The 4s contribution can be written

$$|\psi_{4s}(0)|^2 = \int_0^{E_F} N_s(E) |\psi_s(0, E)|^2 dE \quad (7)$$

where $N_s(E)$ is the number of s -states in the 3d-4s conduction band. Ingalls (1967) performed a modified tight-binding calculation of the 4s wave functions at $\Gamma_1(k=0)$ for several volumes and found

$$|\psi_{\Gamma_1}(0)|^2 = 7.1 a_0^{-3} \quad \text{for } V = 80 a_0^3 \quad (8)$$

and

$$|\psi_{\Gamma_1}(0)|^2 = \text{const } V^{-\gamma} \quad (9)$$

where $\gamma \approx 1.25$. With the assumption that $|\psi_s(0, E)|^2$ equals $|\psi_{\Gamma_1}(0)|^2$, the decrease in the s -like nature of the conduction band being completely represented by the decrease in $N_s(E)$ as k increases, Ingalls obtained

$$|\psi_{4s}(0)|^2 = n_s |\psi_{\Gamma_1}(0)|^2 \quad (10)$$

where $n_s = 0.53$ is the number of s -electrons per iron atom.

The 3s contribution is approximated by using the proportionality found by Watson (1959) and Clementi (1965) between the density of 3s electrons at the nucleus and $\langle nu_m^2 \rangle$

$$|\psi_{3s}(0)|^2 = \beta \langle nu_m^2 \rangle \quad (11)$$

where u_m is the maximum of the radial wave function in the wave function and

$$\langle nu_m^2 \rangle = \int_0^{E_F} N_d(E) u_m^2(E) dE \quad (12)$$

where $\beta = -5.5 a_0^{-2}$. The integral in eqn (12) is performed up to the respective Fermi energy in each half of the band (spin up and spin down) using the linear relationship between $u_m^2(E)$ and E discussed by Ingalls.

Thus for the 3s and 4s contributions we have

$$|\psi(0)|^2 = n_s |\psi_{\Gamma_1}(0)|^2 + \beta \langle nu_m^2 \rangle. \quad (13)$$

Taking the volume derivative of eqn (12) gives

$$\begin{aligned} \frac{d|\psi(0)|^2}{d(\ln V)} = & -n_s \gamma |\psi_{\Gamma_1}(0)|^2 + \beta \frac{\partial \langle nu_m^2 \rangle}{\partial(\ln V)} \\ & + |\psi_{\Gamma_1}(0)|^2 \frac{\partial n_s}{\partial(\ln V)} + \beta \frac{\partial \langle nu_m^2 \rangle}{\partial n_d} \frac{\partial n_d}{\partial(\ln V)}. \end{aligned} \quad (14)$$

Here one sees the expression for $d(\Delta\epsilon)_L$, due to volume scaling, and for $d(\Delta\epsilon)_B$, due to $s \leftrightarrow d$ electron transfer

$$\frac{d(\Delta\epsilon)_L}{d(\ln V)} = \alpha \left[-n_s \gamma |\psi_{\Gamma_1}(0)|^2 + \beta \frac{\partial \langle nu_m^2 \rangle}{\partial(\ln V)} \right] \quad (15)$$

$$\frac{d(\Delta\epsilon)_B}{d(\ln V)} = \alpha \left[|\psi_{\Gamma_1}(0)|^2 \frac{\partial n_s}{\partial(\ln V)} + \beta \frac{\partial \langle nu_m^2 \rangle}{\partial n_d} \frac{\partial n_d}{\partial(\ln V)} \right]. \quad (16)$$

Using the values of $|\psi_{\Gamma_1}(0)|^2$, n_s , γ , and β mentioned above and

$$\frac{\partial \langle nu_m^2 \rangle}{\partial(\ln V)} = 0.03 a_0^{-1} \quad \frac{\partial \langle nu_m^2 \rangle}{\partial n_d} = 0.9 a_0^{-1} \quad (17)$$

gives

$$\frac{d(\Delta\epsilon)_L}{d(\ln V)} = -4.86 \quad (18)$$

$$\frac{d(\Delta\epsilon)_B}{d(\ln V)} = \alpha \left[7.1 \frac{\partial n_s}{\partial(\ln V)} - 4.95 \frac{\partial n_d}{\partial(\ln V)} \right] \text{ mm/sec} \quad (19)$$

where

$$\alpha \equiv [a_0^3 \text{ mm/sec}].$$

Equation (18) can be viewed as an alternative to eqn (6), which gave a rough value of $d(\Delta\epsilon)/d(\ln V)$ from volume scaling alone, and it will be used instead of eqn (6). To obtain agreement between these equations we would need $\alpha = -0.35 a_0^3 \text{ mm/sec}$ which is significantly different from the value of $\alpha = -0.47 a_0^3 \text{ mm/sec}$ found above.

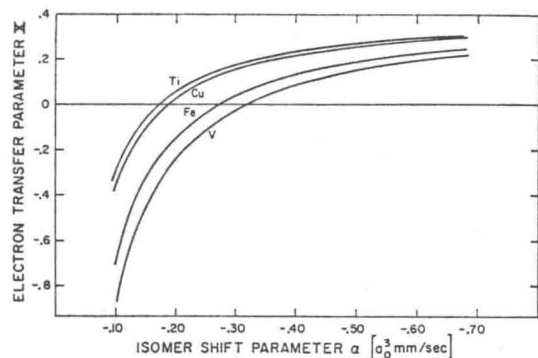
By combining the theory with the experimental measurements and assuming the total number of electrons in the combined 4s-3d band is constant, we obtain:

$$\frac{d(\Delta\epsilon)}{d \ln V} = -4.86\alpha + 12.05\alpha X = 1.32 \quad (20)$$

where

$$X = \frac{\partial n_s}{\partial \ln V} = -\frac{\partial n_d}{\partial \ln V}. \quad (21)$$

This relationship is plotted in Fig. 10.

FIG. 10. α versus X .

While the data do not permit one to fix the value either of α or of X , we can state that they should be related to each other as shown. For values of α less than about $-0.28 \text{ a}_0^3 \text{ mm/sec}$ (that is greater in magnitude than this number), X is positive which corresponds to transfer of electrons from the s to the d part of the conduction band with increasing pressure. Alternatively, the values for α suggested by Siminek and Sroubec (1967) or by Gol'danski (1963) or Danon (1966) would correspond to relatively large d to s transfer. Stern (1955) has found that as the volume decreases the d band lowers in energy with respect to the s band, making an s to d transfer energetically favourable. Unless one establishes a serious error in Stern's calculation, this is strong evidence in favour of a smaller, that is a more negative, value of α .

In Fig. 10 are also plotted values of α versus X for vanadium, copper, and titanium. Vanadium has the b.c.c. structure while the other two are close packed (b.c.c. and h.c.p. respectively). These are typical of the results for the classes of systems. In general, the close-packed systems exhibit a stronger tendency for s to d transfer than do the b.c.c. metals. This illustrates the basic difference in the effect of pressure on the band structure of these two classes of metals.

2. Ionic Compounds

Figure 11 shows isomer shifts as a function of pressure for a series of typical high spin ferrous and ferric compounds. Insofar as the classification is meaningful, these would be classified as "ionic", and from the figure several facts are apparent. All compounds show a measurable

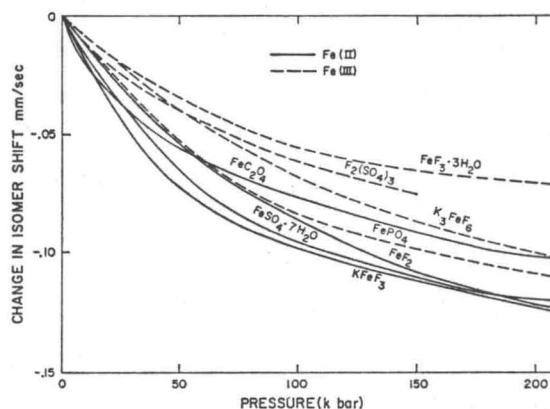


FIG. 11. Isomer shift versus pressure—high spin ferrous and ferric compounds.

increase in electron density at the iron nucleus with increasing pressure. On the average, the ferrous compounds show a measurably larger effect than do the ferric which is almost certainly not due to any consistent difference in compressibility. The effect in the ferrous ion is some 10–12% of the difference between normal ferrous and ferric ions in 150 kb, which represents a significant change in electronic configuration in this range.

In both cases these compounds and other relatively ionic materials such as FeCl_3 and FeBr_3 group into two quite narrow ranges. If the change with pressure were due primarily to electron transfer between ligand and metal, one would expect a much larger variation from ligand to ligand than is observed. It therefore seems reasonable to attribute the pressure effect to deformation of the metal ion wave functions. Simanek and Sroubec (1967) attribute the change with pressure for the ferrous ion entirely to compression of the " s " electrons, increasing the nuclear overlap. Champion *et al.* (1967) attribute the change for both ferrous and ferric ions to reduced shielding of the $3s$ electrons due to the spreading of the $3d$ orbitals discussed earlier. The ferric ions show a smaller change because there are only five $3d$ electrons in this case.

It seems most probable that neither of these factors is negligible. At present there is no apparent way to establish with certainty which is more important. The Simanek and Sroubec approach used as the sole

mechanism for the pressure change gives a value of α which seems inconsistent with the data for metallic iron. At present the authors consider the change in shielding as probably the most important factor, but this is a tentative judgment, and considerable further study is needed.

It seems difficult to reconcile the narrow range of isomer shifts and the consistent change with pressure for both ferrous and ferric compounds with results of molecular orbital calculations using LCAO orbitals and a Mulliken population analysis. These indicate relatively small differences in electron distribution for ferrous and ferric ions with the same ligand, and, for the ferric ion in particular, a high covalency with the electron distribution strongly dependent on the ligand. These methods are probably particularly applicable to atoms with a relatively small number of electrons. It is also well known that one can get very satisfactory calculations of energies and of energy differences between states of a system using wave functions which are not a particularly accurate description of the true orbital. It may be that a linear combination of atomic orbitals using free ion wave functions is a rather inaccurate description of the wave function amplitude at the nucleus.

3. Covalent Compounds

Figure 12 exhibits the change in isomer shift with pressure for four compounds which show a high degree of electron sharing between ligand and metal. There is a very large change in isomer shift with pressure

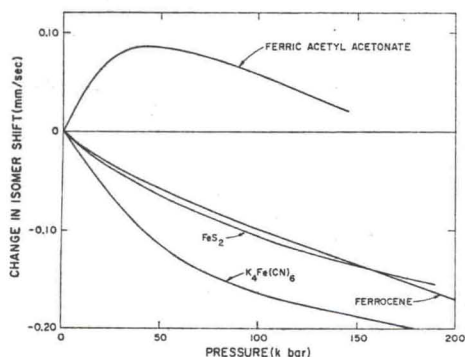


FIG. 12. Isomer shift versus pressure—"covalent" compounds.

for ferrocene, pyrites and potassium ferricyanide. This is not a compression effect, that is, it is not a result of especially high compressibility. The pyrites crystal is known to be relatively incompressible, and surely neither the ferrocene molecule nor the ferrocyanide molecular ion would show a large change in bond length with pressure. Also shown is ferric acetyl acetonate which actually exhibits a decrease in electron density with increasing pressure in the low pressure region with a reversal at higher pressures.

In these cases, in addition to changes in shielding and compression of the s wave functions, there must be significant change in orbital occupation with pressure. A calculation for ferrocene by Vaughan and Drickamer (1967a) indicates that at least one third of the change with pressure for that compound can be accounted for by changes in electron distribution among the orbitals. Each compound, however, requires an individual analysis so that no generalizations are possible.

B. QUADRUPOLE SPLITTING

As mentioned earlier, an electric field gradient at the nucleus can interact with nuclear states of spin equal to or greater than one, partially removing their degeneracy. The Mössbauer resonance is one of a variety of tools for investigating this effect. Here we shall discuss only briefly some high pressure results for a few compounds of iron. There are two possible sources of an electric field gradient at a transition metal nucleus. Firstly, the electrons in the partially filled $3d$ shell may exhibit less than spherical symmetry and, as mentioned earlier, this will be true, in general, for high spin ferrous or for low spin ferric compounds (see Fig. 4). Secondly, the ligands may exhibit less than cubic symmetry and thus impose an electric field gradient at the nucleus. Where the first effect is present it will dominate, since quadrupolar forces are short range and the effective radius of the $3d$ shell is much smaller than the average ligand-metal distance.

For preciseness, let us consider a high spin ferrous ion in an octahedral field. If the three t_{2g} levels are truly degenerate the orbital of the sixth electron will be spherically distributed and there will be no quadrupole splitting. As soon as the degeneracy is removed even by a very small splitting, the electron will not have an equal probability of being in the three t_{2g} states and a relatively large splitting results. Most high spin ferrous compounds exhibit a splitting of 2-3 mm/sec at room temperature. As one lowers the temperature one would expect the probability for occupation of the lowest level to increase by a Boltzmann factor and, in fact, the splitting does increase. If as the pressure

increases the energy difference between states increases, one would expect the splitting to increase with pressure and ultimately to "saturate" when only the ground state had significant occupation probability. This indeed happens for many high spin ferrous systems as is illustrated in Fig. 13 for ferrous oxalate. There is a large number

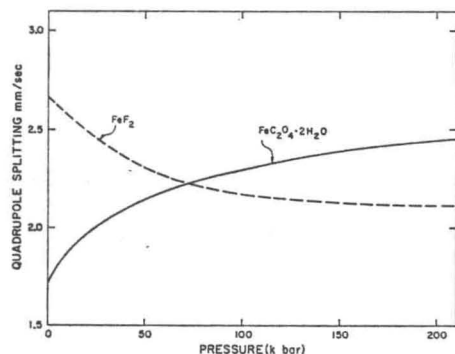


Fig. 13. Quadrupole splitting versus pressure—ferrous compounds.

of other examples in the literature (for example Champion *et al.*, 1967a). However, pressure may act to reduce the splitting among the t_{2g} levels and partially to equalize their occupation probability, thus reducing the quadrupole splitting as is shown for FeF_2 , also in Fig. 13. For no change in relative distortion, it can be shown that the distorting field should increase as r^{-3} (or this term times a function of angle). Thus, one would expect more examples of increasing than of decreasing quadrupole splitting with increasing pressure for high spin ferrous compounds, and this is what is observed.

For high spin ferric compounds in a strictly cubic environment one would expect no quadrupole splitting. In almost all cases there appears to be some distortion, either trigonal, tetrahedral, or rhombohedral, since most high spin ferric compounds show small but measurable quadrupole splitting (0.3–0.6 mm/sec). Since the ferric quadrupole splitting responds directly to the ligand-metal distance (as r^{-3}), one would expect a large pressure effect. As typical data for K_3FeF_6 and $\text{FeF}_3 \cdot 3\text{H}_2\text{O}$ show (Fig. 14), this is indeed observed. Frequently, the increase in splitting with pressure is more rapid than r^{-3} , indicating that there is a tendency to increase the non-cubic component of the field with pressure.

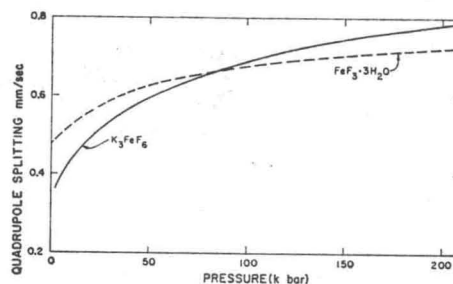


Fig. 14. Quadrupole splitting versus pressure—ferric compounds.

No general discussion of low spin compounds is possible, since these involve strong chemical binding and complex orbital occupation, but there are some special cases (not necessarily low spin) which deserve discussion. Firstly, ferrocene, which was mentioned briefly in the section on isomer shifts, is one of the most interesting and most thoroughly studied organometallic compounds. Iron is sandwiched between two C_5H_5 (dicyclopentadiene) rings to form a very stable molecule. The effect of pressure has been studied on both the optical and the Mössbauer spectrum of this compound (Zahner and Drickamer, 1961; Vaughan *et al.*, 1967a).

There have been a number of theoretical treatments of the electronic structure of ferrocene, but that of Dahl and Ballhausen (1961) forms the best basis for discussion of pressure effects. The application is discussed in detail by Vaughan and Drickamer (1967a). By estimating bond compressibilities from bond-force constants one can estimate orbital occupation as a function of pressure. One can show that there is a significant electron transfer from metal to ligand in the $e_{2g}(d \pm 2)$ orbitals with increasing pressure, and a reverse flow in the $e_{1g}(d \pm 1)$ orbitals. Using the treatment of Höfflinger and Voitländer (1963), one can show that this would predict a marked decrease in quadrupole splitting with increasing pressure. As shown in Fig. 15, the experimental and predicted splittings are in essentially quantitative agreement; as shown in Vaughan and Drickamer (1967a), the theory also predicts correctly the behaviour of the low energy optical transition as a function of pressure.

The compound $\alpha\text{-Fe}_2\text{O}_3$ is one of the most studied of iron compounds. It has a rhombohedral crystal structure with each iron located in an octahedron of oxygen ions, although the iron is about 0.06 Å above the

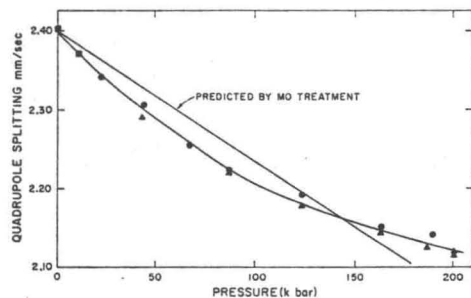
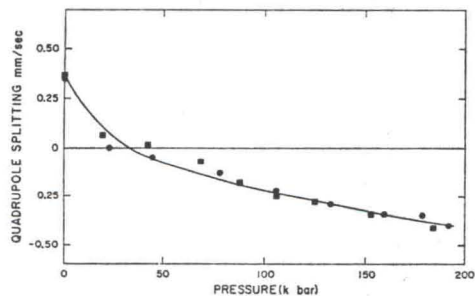


FIG. 15. Quadrupole splitting versus pressure—ferrocene.

centre of the octahedron. The material is antiferromagnetic below 950°K; from 950°K to about 260°K the internal magnetic field is perpendicular to the (111) body diagonal of the unit cell. Below this temperature (called the Morin temperature) it reorients through 90° and becomes parallel to the body diagonal. In such a crystal the equation for the quadrupole splitting contains a factor $(3 \cos^2\theta - 1)$ which changes from -1 to $+2$ as one goes from a temperature above to one below the transition. This change in quadrupole splitting as a function of temperature has been observed by Ono and Ito (1962).

The effect of pressure on the quadrupole splitting has been observed by Vaughan and Drickamer (1967b) using Mössbauer resonance; the low pressure region has also been studied by Worlton *et al.* (1967) using neutron diffraction. Figure 16 shows the observed splitting as a function of pressure. A sign change is obtained at about 30 kb. This has

FIG. 16. Quadrupole splitting versus pressure—Fe₂O₃.

the qualitative features of a Morin transition, although there are several anomalous points. The transition is smeared out over a considerable range of pressure and in this transition region one does not observe the peak broadening which Ono and Ito saw in the temperature region where two phases were present. Finally, in the high pressure region the magnitude of the splitting is not twice the atmospheric pressure value. These observations can be explained by a small movement of the iron ion in the oxygen octahedron. It is possible to show that a shift of only 0.04 Å in the position of the iron in a direction towards the centre of symmetry would be enough to cause the quadrupole splitting to go to zero. A slight shift accompanied by the Morin transition would account for the results. Worlton and Decker (1968) have shown that a more plausible argument involves the continuous change of the angle between the antiferromagnetic axis and the (111) axis of the crystal.

C. MAGNETISM

In the introduction it was pointed out that a magnetic field at the iron nucleus removed the degeneracy of both the ground state and the excited state. When one considers the selection rules, one can account for the observed six line spectrum. The changes in splitting of pairs of these lines with pressure measure the change in magnetic field. To date there have been only a limited number of Mössbauer resonance studies of magnetic fields at high pressure. We shall discuss briefly only two cases: ferromagnetism in iron, cobalt and nickel, and antiferromagnetism in cobalt oxide.

The magnetic field in iron as a function of pressure has been studied by Pound *et al.* (1961), Nicol and Jura (1963), Pipkorn *et al.* (1964), and Moyzis and Drickamer (1968a). A plot is shown in Fig. 17; the solid line in the figure represents the results of zero field n.m.r. measurements by Litster and Benedek (1963). It is interesting to see the very close agreement to 60 kb, the limit of the n.m.r. measurements, as this represents a check on both measurements but also yields additional information. The n.m.r. measurements are sensitive only to atoms at the surface of a domain, while Mössbauer resonance reflects the average field of all of the atoms in the domain. Apparently, the effects of pressure are very uniform throughout the domain. It should also be mentioned that the high pressure Mössbauer studies have shown that the high pressure (h.c.p.) phase of iron is paramagnetic at least at room temperature.

The magnetic field in nickel and in cobalt has been studied as a function of pressure, using ⁵⁷Fe produced by the decay of ⁵⁷Co as a probe by

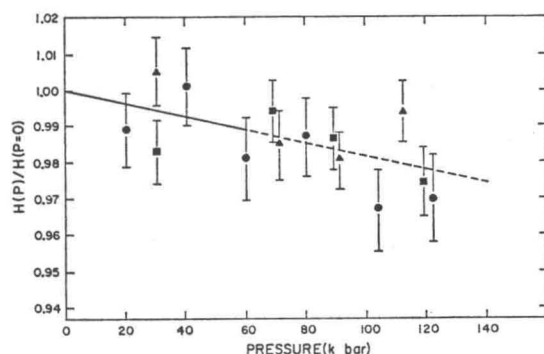
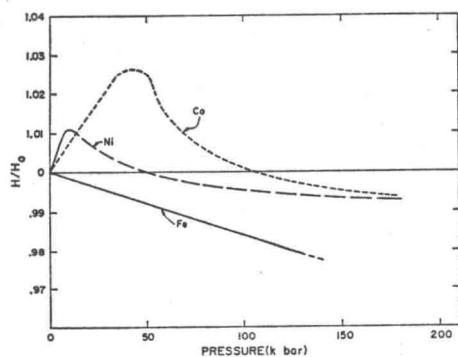


FIG. 17. Magnetic field versus pressure—iron.

Drickamer *et al.* (1965) and in nickel by Raimondi and Jura (1967). Zero field n.m.r. measurements in cobalt as a function of pressure have been reported by Jones and Kaminov (1960), Samara and Anderson (1963) and by Anderson (1965). In Fig. 18 are shown the smoothed values for iron in cobalt and nickel, compared with the data for pure iron discussed above. In both nickel and cobalt there is a distinct increase in magnetic field with pressure in the low pressure region, in distinct contrast to iron. In nickel there is a maximum of about 5–10 kb and in cobalt about 40–60 kb, and at higher pressures the field decreases as in iron.

FIG. 18. Magnetic field versus pressure— ^{57}Fe in cobalt and nickel.

Magnetism in metals and alloys is a very complex phenomenon, especially from the atomic viewpoint. There are a number of theories and no general agreement about many basic points, for example the degree to which the magnetic electrons are bound or itinerate. The theory has not advanced to the point where there is any really acceptable explanation of these pressure effects.

Cobalt oxide (CoO) at room temperature and atmospheric pressure is a cubic paramagnetic crystal with the sodium chloride (f.c.c.) structure. At 291°K it becomes antiferromagnetic, the transition being accompanied by a slight tetragonal distortion. The magnetic field has been measured as a function of temperature by Wertheim (1961) and Bearden *et al.* (1964); their results are represented on the left-hand side of Fig. 19. As one increases the pressure beyond 20 kb at 298°K , a magnetic field appears and increases with increasing pressure, as is shown on the right hand side of Fig. 19 from Coston *et al.* (1966).

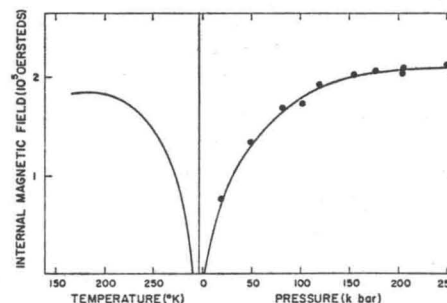


FIG. 19. Magnetic field versus temperature and pressure—cobalt oxide.

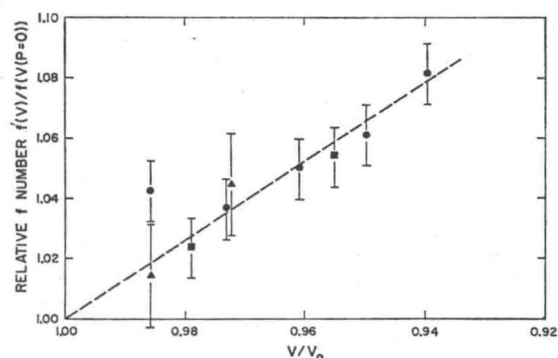
Since antiferromagnetism in materials like CoO is described in terms of superexchange, which depends strongly on overlap of wave functions of adjacent ions, the study of the field as a function of interatomic distance at constant temperature should be a very fruitful field of investigation.

It has been emphasized throughout this section that the initiation of ferro- or antiferromagnetism in a solid is heralded by the appearance of a six line spectrum. The observation of the appearance and disappearance of this six line spectrum as a function of pressure at constant temperature, or as a function of temperature at constant pressure, makes a very useful way of determining Curie or Néel temperatures as a function of pressure.

D. THE MEASUREMENT OF f NUMBER

While the f number, the fraction of recoilless decays, is a very basic quantity in Mössbauer theory, its quantitative experimental evaluation, even at one atmosphere, is very difficult. The main purpose of such a measurement is to study the localized vibrational structure in the solid in the neighbourhood of the decaying atom. As we shall see, in transition metals in the first order this does not differ greatly from the vibrational structure of the host.

The extensive high pressure measurements involve ^{57}Co (^{57}Fe) as a dilute solute in copper, vanadium and titanium. These have respectively, the f.c.c., and b.c.c., and h.c.p. structures, although titanium undergoes a transition near 80 kb. We shall be concerned here only with the measurement of relative f 's, that is the value of f relative to its value at one atmosphere and the same temperature (294°K). Figures 20 and 21 show plots of f/f_0 versus $\Delta V/V_0$ for copper and vanadium

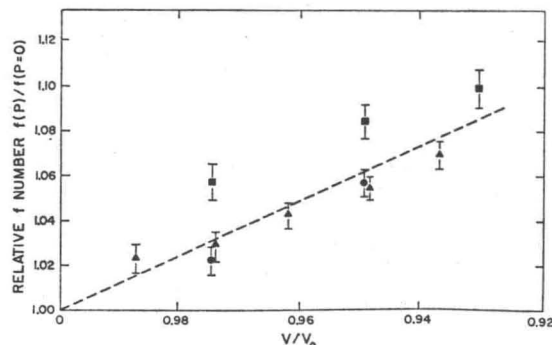
FIG. 20. f/f_0 versus $\Delta V/V_0$ —copper.

from Moyzis and Drickamer (1968a). The titanium data are more scanty, but similar in nature. One sees that within the accuracy of the data the relationship is linear.

From eqn (3) it is convenient to write:

$$\frac{\partial \ln f}{\partial \ln V} = -\gamma Y \quad (22)$$

where $\gamma = -\frac{\partial \ln \theta}{\partial \ln V}$ is the Grüneisen constant,

FIG. 21. f/f_0 versus $\Delta V/V_0$ —vanadium.

and

$$Y = \frac{6E_r}{k\theta} \left[\frac{1}{4} - \frac{1}{\rho^{\theta/T} - 1} + 3 \left(\frac{T}{\theta} \right)^2 \int_0^{\theta/T} \frac{x dx}{\rho^x - 1} \right].$$

It should be noted that the dependence on ω ($\langle \omega^{-2} \rangle$) is the same as for X-ray scattering but differs from the specific heat which varies as $\langle \omega^2 \rangle$.

The experimental results give:

$$\frac{\partial \ln f}{\partial \ln V} \Big|_{\text{Cu}} = -1.283 \quad (23)$$

$$\frac{\partial \ln f}{\partial \ln V} \Big|_{\text{V}} = -1.380 \quad (24)$$

$$\frac{\partial \ln f}{\partial \ln V} \Big|_{\text{Ti}} = -0.843. \quad (25)$$

From these results it is possible to calculate a value for the characteristic temperature θ which can be corrected to apply to the host lattice by the relationship:

$$\theta_H = \left(\frac{m'}{m} \right)^{1/2} \theta_f \quad (26)$$

where $\theta_H = \theta$ of host, $\theta_f = \theta$ obtained from experiment, m, m' = mass of host and impurity atom.

Since the relationship of Figs 20 and 21 is linear, the above calculation can be assumed to apply at an average pressure of 50 kb. One

can calculate the one atmosphere value from

$$\theta_0 = \left(\frac{V_p}{V_0} \right)^\gamma \theta_p \quad (27)$$

where γ is the Grüneisen constant.

The resultant values for θ are listed in Table I. Since the f number measures a mean value of $\langle \omega^{-2} \rangle$ where ω is the lattice vibrational

TABLE I. Mössbauer and Grüneisen constants for copper, vanadium and titanium

| Element | 50 kb | | Atmospheric | | γ |
|---------|------------------------------|--|------------------------------|--|----------|
| | $\theta_f(^{\circ}\text{K})$ | $\theta_{\text{host}}(^{\circ}\text{K})$ | $\theta_f(^{\circ}\text{K})$ | $\theta_{\text{host}}(^{\circ}\text{K})$ | |
| Cu | 350 ± 14 | 331 ± 14 | 327 ± 14 | 309 ± 14 | 1.998 |
| V | 268 ± 10 | 284 ± 11 | 258 ± 10 | 274 ± 11 | 1.257 |
| Ti | 339 ± 35 | 370 ± 40 | 321 ± 35 | 350 ± 40 | 1.232 |

frequency, it is most meaningful to compare these θ 's with θ obtained from X-ray diffraction measurements. Unfortunately, this can only be done for copper. Table II summarizes the available data for this metal. It can be seen that the X-ray results are in excellent agreement with the predictions from high pressure Mössbauer data.

TABLE II. θ_D from X-ray measurements for copper

| Investigators | Debye parameter ($^{\circ}\text{K}$) |
|---------------------------------|--|
| Owen and Williams (1947) | 314 |
| Burie (1956) | 299 |
| Chipman and Paskin (1959) | 307 (327) ^a |
| Flinn <i>et al.</i> (1961) | 322 |
| Graevskaya <i>et al.</i> (1965) | 310 |

^a Parenthetic value corrected for one and two phonon generation.

A direct comparison of these results with other data for vanadium is more difficult. The values of θ available are from low temperature specific heat measurements and are listed in Table III. It should be kept in mind that vanadium is superconducting below 5.4°K so that measurements must be made in a field 5–10 kgauss. Further, a large correction for electronic specific heat is necessary. The results in Table IV show a rather distinct trend with sample purity, with the more impure samples agreeing with our result. This is perhaps

TABLE III. θ_D from specific heat measurements for vanadium

| Investigators | Sample purity (%) | $\gamma_C (^{\circ}\text{K})$ |
|------------------------------|-------------------|-------------------------------|
| Wolcott (1955) | > 99.98 | 380 |
| Worley <i>et al.</i> (1955) | sample 1: 99.50 | 308 |
| | sample 2: 99.80 | 273 |
| Corak <i>et al.</i> (1956) | ≈ 99.80 | 338 |
| Clusius <i>et al.</i> (1960) | 99.50 | 425 ^a |
| Radebaugh and Keesom (1966) | > 99.99 | 382 |

^a Experiment performed in temperature range 11–23°K.

reasonable, as our samples contained ^{57}Co (^{57}Fe) impurity. It must be remembered that θ_C is a distinct function of temperature and may be 50° or more lower at room temperature.

For titanium, Wolcott (1957) and Johnson and Kothan (1953) have made C_v measurements over a long temperature range. At low temperatures they obtain $\theta = 430^{\circ}\text{K}$ and near room temperature a value of 360°K, in very good agreement with these results.

The results for these three metals demonstrate that, to a good approximation, γ is independent of density at least to 100 kb, which validates the Grüneisen equation of state over this range and permits the prediction of θ as a function of pressure to 100 kb at least.

TABLE IV. Constants A and B for relationship $K = AP_B$

| Compound | A | B |
|------------------------------------|-------|------|
| FeCl_3 | 0.265 | 0.56 |
| FeBr_3 | 0.076 | 0.43 |
| KFeCl_4 | 0.092 | 0.50 |
| FePO_4 | 0.078 | 0.46 |
| Phosphate Glass | 0.048 | 0.31 |
| Ferric Acetate (418°K) | 0.022 | 0.98 |
| Ferric Citrate | 0.112 | 0.35 |
| $\text{K}_3\text{Fe}(\text{CN})_6$ | 0.109 | 2.06 |

E. CONVERSION OF Fe^{III} TO Fe^{II}

As has been emphasized in the earlier sections, the Mössbauer spectra of high spin ferrous and high spin ferric iron are entirely different, both as regards isomer shift and quadrupole splitting. It is therefore easy to discern the appearance of one oxidation state in the

presence of the other, and to estimate the relative amounts of the two states from computer fit areas. Although the difference in low spin states is less spectacular, the calculation is still possible. Perhaps the most remarkable of the high pressure Mössbauer observations is that ferric iron reduces to ferrous iron with increasing pressure in a wide variety of compounds, and that this is essentially a reversible process. This has been discussed in a series of articles including Champion *et al.* (1967), Champion and Drickamer (1967a, b), Lewis and Drickamer (1967a), and Fung (1968).

As an example, a series of spectra for FeCl_3 are shown in Figs 22(a, b). The process reverses upon release of pressure, but with considerable hysteresis. On removing the pellet and powdering the sample one almost always recovers the atmospheric spectrum. A greater or lesser degree of conversion has been observed in FeCl_3 , FeBr_3 , KFeCl_4 , FePO_4 , $\text{Fe}_2(\text{SO}_4)_3$, $\text{Fe}(\text{NCS})_3$, $\text{Fe}(\text{NH}_3)_6\text{Cl}_3$, $\text{K}_3\text{Fe}(\text{CN})_6$, ferric citrate, basic ferric acetate, ferric acetyl acetonate, ferric oxalate, various hydrates, hemin and hematin.

The form of the pressure dependence is essentially always the same, as is illustrated in Figs 23 and 24. If one defines an equilibrium constant $K = C_{\text{II}}/C_{\text{III}}$, then

$$K = AP^B \quad (28)$$

where A and B are independent of pressure. Typical values for these constants are shown in Table IV. It has been shown that one is observing true equilibrium and not the results of slow kinetics by the fact that successive spectra run at the same pressure are substantially identical.

The reaction is almost always endothermic, that is the conversion increases with increasing temperature, although in the case of hemin the conversion actually decreases with increasing temperature. The heat of reaction generally is in the range 0.1–0.3 eV, and usually increases with increasing temperature. For the most ionic systems the heat of reaction does not depend significantly on pressure, but in more covalent materials it may increase or decrease sharply with increasing pressure.

One is faced with two problems in discussing these results: why does the electron from ligand to metal take place, and why does the reaction have the observed pressure dependence, that is why does one not obtain discontinuous ferric to ferrous conversion at some pressure.

As discussed in the introduction, it is possible to excite an electron optically from the non-bonding ligand levels to the lowest antibonding metal levels ($t_{2u} \rightarrow t_{2g}$ in octahedral symmetry). This optical charge

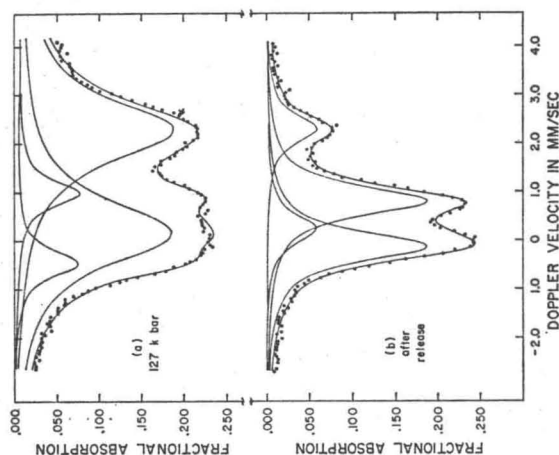


Fig. 22b. Mössbauer spectra for FeCl_3 continued.

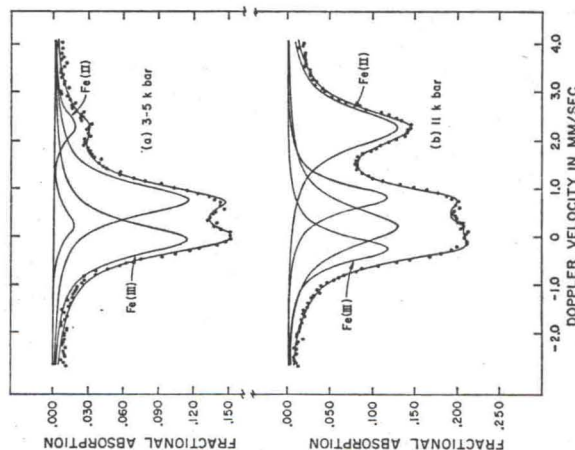
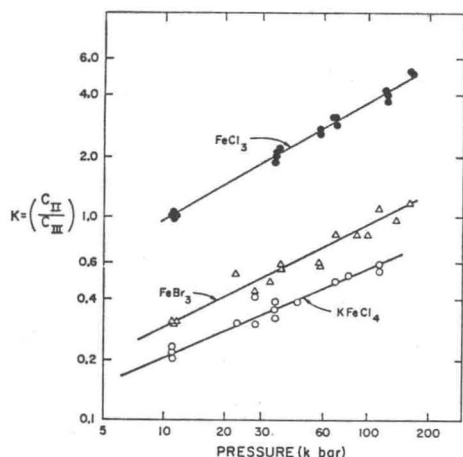
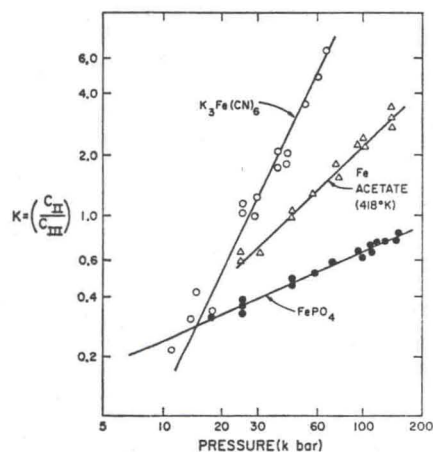


Fig. 22a. Mössbauer spectra for FeCl_3 .

FIG. 23. $\ln K$ versus $\ln P$ — FeCl_3 , FeBr_3 and KFeCl_4 .FIG. 24. $\ln K$ versus $\ln P$ — FePO_4 , $\text{K}_3\text{Fe}(\text{CN})_6$ and basic ferric acetate.

transfer peak normally has an energy of 3–6 eV, with a long low energy tail which may extend through the visible and even into the infrared part of the spectrum. As indicated earlier, a red shift (shift to lower energy) of one-half to 1 eV in 100 kb is observed experimentally, and can be explained theoretically; however this is of course not sufficient to move the optical peak to zero energy. The high pressure transition observed by the Mössbauer studies is, however, a thermal transition which takes place sufficiently slowly so that the atomic coordinates can assume their new equilibrium values, whereas an optical transition must take place vertically on a configuration diagram, according to the Franck-Condon principle. The situation is illustrated in a typical diagram in Fig. 25. The horizontal configuration coordinate is typically some vibrational mode of the system (metal plus ligands) which

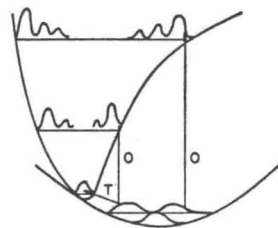


FIG. 25. Schematic configuration coordinate diagram. O = optical transition, T = thermal transition.

permits the rearrangement. The observed tail on the charge transfer peak is consistent with a very steep slope of the side of the excited-state potential well above the centre of the ground-state well, and accounts for the small thermal energy necessary for the transition. The diagram also explains the temperature coefficient of the equilibrium constant, as there is a thermal distribution for transfer of electrons from the ground to the excited electronic level, and in addition a distribution of electrons among the vibrational levels of the ground state with increasing temperature.

There remains the problem of the pressure dependence of the conversion. Qualitatively, one can see why the conversion does not go to completion at a given pressure as follows. When electron transfer takes place, one creates a ferrous ion in a ferric site plus a free radical or radical ion. (The excitation may also be smeared out over the nearest neighbour ligands.) There is thus a transfer of charge, a change of

volume and a distortion. This affects the neighbouring complexes, distorting the potential wells in such a way as to make electron transfer less favourable. With increasing pressure the excited state is lowered further and one obtains more conversion, but with further increase in local strain. The sluggishness and hysteresis with which the process reverses on release of pressure can be associated with the stored up strain.

The situation can be described thermodynamically:

$$K = \exp(-\Delta G/RT) \quad (29)$$

$$\frac{\partial \ln K}{\partial \ln P} = -\frac{P\Delta\bar{V}}{RT} = \frac{P(\bar{V}^{\text{III}} - \bar{V}^{\text{II}})}{RT} \quad (30)$$

where \bar{V}^{III} and \bar{V}^{II} refer to the partial molar volumes of the ferric and ferrous sites plus their associated ligands.

From our empirical observation

$$\frac{\partial \ln K}{\partial \ln P} = B \quad (31)$$

where B is a constant. One can rearrange eqn (29), remembering that $K = C_{\text{II}}/1 - C_{\text{II}}$. Then

$$\frac{\partial \ln C_{\text{II}}}{\partial \ln P} = \frac{P(\bar{V}^{\text{III}} - \bar{V}^{\text{II}})}{RT} (C_{\text{III}}). \quad (32)$$

Thus, the fractional increase in conversion with fractional increase in pressure is proportional to C_{III} , the number of sites available for conversion. The proportionality coefficient is the work necessary to form a ferrous site from a ferric site, measured in thermal units (that is in units of RT). It is entirely reasonable that in the first order the dependence would be first order in these variables, and that to the first approximation the coefficient is a constant. Experimentally, it appears that higher order terms are negligible.

F. HIGH PRESSURE MÖSSBAUER STUDIES ON GLASS

An interesting application of high pressure Mössbauer resonance is the investigation of the structure of glass. Lewis and Drickamer (1968) and Kurkjian and Sigety (1964) have made extensive studies, correlating the atmospheric Mössbauer spectrum of ferric ions with the site symmetry. Tischer and Drickamer (1962) have studied the effect of pressure on the optical spectra of a number of transition metal ions

in various glasses. The work discussed here involves Mössbauer studies of Fe^{III} and Fe^{II} ions in a phosphate and in a silicate glass.

The phosphate glass consists of chains of PO_4^- tetrahedra with little crosslinking, in contrast to the silicate glass discussed below. Both the ferric and the ferrous ions are in octahedral sites in the phosphate glass. High pressure Mössbauer resonance studies have also been made on FePO_4 and $\text{Fe}_3(\text{PO}_4)_2$ in the crystalline state (Champion *et al.*, 1967a). The Fe^{III} ion in the glassy medium behaved in much the same way as it did in the crystal. This is illustrated in the change in isomer shift and quadrupole splitting for the Fe^{III} ion in Figs 26 and 27.

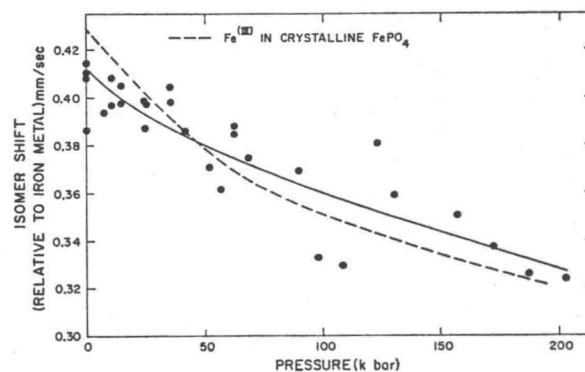


FIG. 26. Isomer shift versus pressure— Fe^{III} in phosphate glass.

The ferric ion reduced to the ferrous state with pressure in the glass as it did in the crystal but with different coefficients A and B . These are listed in Table IV in the previous section. The behaviour of the Fe^{II} ion in the phosphate glass was also quite similar to that in the crystal.

The silicate glass, in addition to chains and rings, includes three dimensional networks. Kurkjian and Sigety (1964) have shown that the ferric ion is in a tetrahedral site in silicate glass, while Tischer and Drickamer (1962) indicate that the ferrous ion is in a loose octahedral site. Weyl (1951) shows that the ferric ion is both a network former and a network modifier in silicate glass, that is it can replace a silicon or be in an interstice. Ferrous ion is always a network modifier.

The isomer shift for Fe^{III} ion is shown as a function of pressure in Fig. 28. One observes an increase with increasing pressure in the low

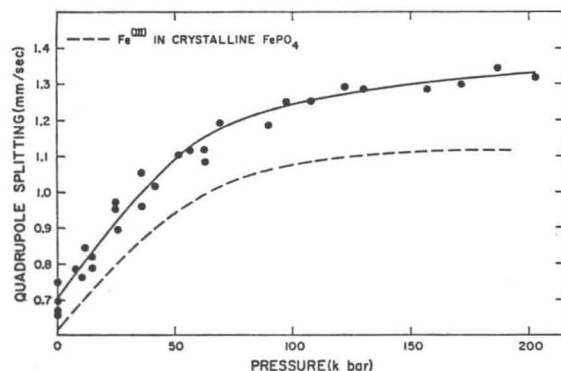


FIG. 27. Quadrupole splitting versus pressure—Fe^{III} in phosphate glass.

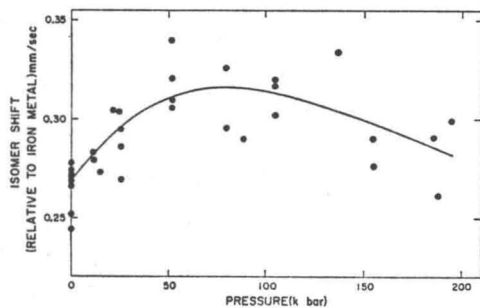


FIG. 28. Isomer shift versus pressure—Fe^{III} in silicate glass.

pressure region, a maximum at about 60 kb, and a decrease at higher pressures. The rather low initial value is consistent with a high degree of covalency. Apparently, in the low pressure region changes in orbital occupation dominate, while at high pressure the deformation of the wave functions controls and gives an increase in electron density at the nucleus with increasing pressure. The quadrupole splitting increases very rapidly with pressure, especially at lower pressures, indicating that substantial changes in site symmetry and/or electronic structure occur in the lower pressure region. No tendency for Fe^{III} to reduce to Fe^{II} was observed.

The ferrous ion, in a loose octahedral site, shows virtually no change in isomer shift with pressure. The quadrupole splitting behaves in an unusual manner as shown in Fig. 29; at low pressure there is a small but distinct drop, then a rise. Obviously there is a combination of site compression, change of symmetry, and electron redistribution at these sites. A run was also made with radioactive ⁵⁷Co introduced as cobaltous ion in silicate glass, and it, of course, does decay to ferrous ion. As can be seen in Fig. 29, the quadrupole splitting behaved

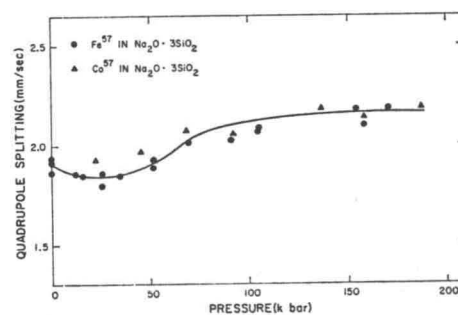


FIG. 29. Quadrupole splitting versus pressure—Fe^{II} in silicate glass.

identically to the ordinary ferrous ion, while the isomer shift parallels the behaviour of ordinary ferrous ion but at considerably higher electron density. The only apparent difference was that the cobalt formed a very dilute solution, while the iron was present in about 5% concentration.

In summary, it can be said that both Fe^{III} and Fe^{II} sites in phosphate glass behave very much like those in crystalline phosphates. In silicate glass the Fe^{III} sites exist in tetrahedral sites with considerable covalency and undergo significant change in orbital occupation in the low pressure region. At the ferrous sites, which are of open octahedral symmetry, there is considerable distortion with increasing pressure.

ACKNOWLEDGEMENT

It is a pleasure to acknowledge the support of the United States Atomic Energy Commission and the collaboration of many students and Research Associates in this work.

REFERENCES

- Anderson, D. H. (1965). *Bull. Am. phys. Soc.* **10**, 75.
- Ballhausen, C. J. (1962). "Introduction to Ligand Field Theory." McGraw-Hill, New York.
- Ballhausen, C. J. and Gray, H. B. (1965). "Molecular Orbital Theory." Benjamin, New York.
- Bearden, A. J., Mattern, P. L. and Hart, T. R. (1964). *Rev. mod. Phys.* **36**, 370.
- Burie, B. (1956). *Acta. Cryst.* **9**, 617.
- Champion, A. R. and Drickamer, H. G. (1967a). *J. chem. Phys.* **47**, 2591.
- Champion, A. R. and Drickamer, H. G. (1967b). *Proc. natn Acad. Sci. U.S.A.* **58**, 876.
- Champion, A. R., Vaughan, R. W. and Drickamer, H. G. (1967). *J. chem. Phys.* **47**, 2583.
- Chipman, D. R. and Paskin, A. (1959). *J. appl. Phys.* **30**, 1992.
- Clementi, E. (1965). *IBM JI Res. Dev. Suppl.* **9**, 2.
- Clusius, K., Franzosini, P. and Piesbergen, V. (1960). *Z. Naturf.* **15a**, 728.
- Corak, W. S., Goodman, B. B., Satterthwaite, C. B. and Wexler, A. (1956). *Phys. Rev.* **102**, 656.
- Coston, C. J., Ingalls, R. L. and Drickamer, H. G. (1966). *Phys. Rev.* **145**, 876.
- Dahl, J. P. and Ballhausen, C. J. (1961). *K. danske Vidensk. Selsk. Skr.* **33**, 39.
- Danon, J. (1966). In "Application of the Mössbauer Effect in Chemistry and Solid State Physics." International Atomic Energy Agency, Vienna.
- DeBrunner, P., Vaughan, R. W., Champion, A. R., Cohen, J., Moyzis, J. A. and Drickamer, H. G. (1966). *Rev. sci. Inst.* **37**, 1310.
- Drickamer, H. G. (1963). In "Solids under Pressure." ed by W. Paul and D. Warschauer. McGraw-Hill, New York.
- Drickamer, H. G. (1965). In "Solid State Physics." Vol. 17, ed. by F. Seitz and D. Turnbull. Academic Press, New York.
- Drickamer, H. G., Ingalls, R. L. and Coston, C. J. (1965). In "Physics of Solids at High Pressures." ed. by C. T. Tomazuka and R. M. Emrick. Academic Press, New York.
- Edge, C. K., Ingalls, R. L., Debrunner, P. G., Drickamer, H. G. and Frauenfelder, H. (1965). *Phys. Rev.* **138A**, 729.
- Flinn, P. A., McManus, G. M. and Rayne, J. A. (1961). *Phys. Rev.* **123**, 809.
- Frauenfelder, H. (1963). "The Mössbauer Effect." Benjamin, New York.
- Fung, S. C. (1968). Private communication.
- Gol'danski, V. I. (1963). In "Proceedings of the Dubna Conference on the Mössbauer Effect." Consultation Bureau Enterprises, New York.
- Graevskaya, Y. I., Iveronova, V. I. and Tarasova, V. P. (1965). *Soviet Phys. Solid St.* **7**, 1083.
- Griffith, J. S. (1964). "The Theory of Transition Metal Ions." Cambridge University Press, Cambridge.
- Höflinger, V. B. and Voiländer, J. (1963). *Z. Naturf.* **18a**, 1065, 1074.
- Housley, R. M. and Hess, F. (1966). *Phys. Rev.* **146**, 517.
- Ingalls, R. L. (1967). *Phys. Rev.* **155**, 157.
- Ingalls, R. L., dePasquali, G. and Drickamer, H. G. (1967). *Phys. Rev.* **155**, 165.
- Johnson, N. L. and Kothan, C. W. (1953). *J. Am. chem. Soc.* **75**, 3101.
- Jones, R. V. and Kaminov, I. P. (1960). *Bull. Am. phys. Soc.* **5**, 175.
- Kurkjian, C. R. and Sigety, E. A. (1964). Proceedings VII Congress on Glasses.
- Lewis, G. K., Jr. and Drickamer, H. G. (1968a). *Proc. natn. Acad. Sci.* **61**, 414.
- Lewis, G. K., Jr. and Drickamer, H. G. (1968b). *J. chem. Phys.* **49**, 3785.
- Litster, J. D. and Benedek, G. B. (1963). *J. appl. Phys.* **34**, 688.
- Maradudin, A. A. (1966). In "Solid State Physics," Vol. 18, ed. by F. Seitz and D. Turnbull. Academic Press, New York.
- Mössbauer, R. (1958a). *Z. Phys.* **151**, 124.
- Mössbauer, R. (1958b). *Naturwissenschaften* **45**, 538.
- Moyzis, J. A. and Drickamer, H. G. (1968a). *Phys. Rev.* **171**, 389.
- Moyzis, J. A. and Drickamer, H. G. (1968b). *Phys. Rev.* **172**, 655.
- Nicol, M. and Jura, G. (1963). *Science N.Y.* **141**, 1035.
- Ōno, K. and Ito, A. (1962). *J. physiol. Soc. Japan* **17**, 1012.
- Orgel, L. E. (1960). "An Introduction to Transition Metal Theory." J. Wiley and Sons, New York.
- Owen, E. A. and Williams, R. W. (1947). *Proc. R. Soc. A* **188**, 509.
- Pipkorn, D., Edge, C. K., Debrunner, P., dePasquali, G., Drickamer, H. G. and Frauenfelder, H. (1964). *Phys. Rev.* **135**, A1604.
- Pound, R. V., Benedek, G. B. and Drever, R. (1961). *Phys. Rev. Lett.* **7**, 405.
- Radebaugh, R. and Keesom, P. H. (1966). *Phys. Rev.* **149**, 209.
- Raimondi, D. L. and Jura, G. (1967). *J. appl. Phys.* **38**, 2133.
- Samara, G. and Anderson, D. H. (1963). *J. appl. Phys.* **35**, 3043.
- Simanek, E. and Stroubeck, Z. (1967). *Phys. Rev.* **163**, 275.
- Slater, J. C. (1965). "Quantum Theory of Molecules and Solids", Vol. 2. McGraw-Hill, New York.
- Stern, F. (1955). Ph.D. Thesis Princeton University (unpublished).
- Tischer, R. E. and Drickamer, H. G. (1962). *J. chem. Phys.* **37**, 1554.
- Vaughan, R. W. and Drickamer, H. G. (1967a). *J. chem. Phys.* **47**, 468.
- Vaughan, R. W. and Drickamer, H. G. (1967b). *J. chem. Phys.* **47**, 1530.
- Vaughan, R. W. (1968). Private communication.
- Walker, L. R., Wertheim, G. K. and Jaccarino, V. (1961). *Phys. Rev. Lett.* **6**, 98.
- Watson, R. E. (1959). Report 12, Solid State and Molecular Theory Group. Massachusetts Institute of Technology (unpublished).
- Wertheim, G. K. (1961). *Phys. Rev.* **124**, 764.
- Wertheim, G. K. (1964). "Mössbauer Effect: Principles and Applications." Academic Press, New York.
- Weyl, W. A. (1951). "Colored Glasses." Society of Glass Technology, Sheffield.
- Wolcott, N. M. (1955). In "Conference de Physique des Basses Temperatures." Inst. International du Froid, Paris.
- Wolcott, N. M. (1957). *Phil. Mag.* **2**, 1246.
- Worley, R. D., Zemansky, M. W. and Boorse, H. A. (1955). *Phys. Rev.* **99**, 447.
- Worlton, T. G. and Decker, D. L. (1968). *Phys. Rev.* **171**, 596.
- Worlton, T. G., Bennion, R. B. and Brugger, R. M. (1967). *Phys. Rev. Lett.* **A24**, 653.
- Zahner, J. C. and Drickamer, H. G. (1961). *J. chem. Phys.* **35**, 375.